Electronic Supplementary Material (ESI) for Journal of Materials Chemistry A.

Electronic Supplemental information (ESI)

Unveiling Interfacial Dynamics and Structural Degradation of Solid Electrolytes in Seawater Battery System

Chanhee Lee,[‡ab] Tae-Ung Wi,[‡a] Wooseok Go,[a] Muhammad Fahmi Rahman,[a] Matthew T. McDowell,[bc] Youngsik Kim,[ad*] Hyun-Wook Lee,[a*]

[a]Department of Energy Engineering, School of Energy and Chemical Engineering, Ulsan National Institute of Science & Technology (UNIST), Ulsan 44919, Republic of Korea

[b]George W. Woodruff School of Mechanical Engineering, Georgia Institute of Technology, Atlanta, GA, USA

[c]School of Materials Science and Engineering, Georgia Institute of Technology, Atlanta, GA, USA

[d]Energy Materials and Devices Lab, 4TOONE Corporation, 50 UNIST-gil, Ulsan 44919, Republic of Korea

[‡]These authors contributed equally to this work.

*Correspondence: ykim@unist.ac.kr (Y.S.K), hyunwooklee@unist.ac.kr (H.W.L)

Supplementary Note

1. Estimation of theoretical equilibrium potentials of seawater batteries.

The electrochemical reactions of seawater batteries involve reduction/oxidation of metallic Na on the anode and the oxygen evolution/reduction reaction (OER/ORR) on the cathode. The theoretical equilibrium potentials at the anode and cathode can be described as follows:

i) Charging process

Anode: $2Na^+ + 2e^- \leftrightarrow 2Na \qquad E^o =- 2.71V_{\ vs\ SHE}$

Cathode: 1) $H_2O \leftrightarrow 2H^+ + \frac{1}{2}O_2 + 2e^- \quad E^o =- 1.23V_{\ vs\ SHE}$

2) $2Cl^- \leftrightarrow Cl_2 + 2e^- \qquad E^o =- 1.36V_{\ vs\ SHE}$

Overall: 1) $2Na^+ + H_2O \leftrightarrow 2Na + 2H^+ + \frac{1}{2}O_2 \ E^o = 3.94V_{\ vs\ Na/Na^+}$

2) $2Na^+ + 2Cl^- \leftrightarrow 2Na + Cl_2 \qquad E^o = 4.07V_{\ vs\ Na/Na^+}$

ii) Discharging process

Anode: $2Na \leftrightarrow 2Na^+ + 2e^- \qquad E^o = 2.71V_{\ vs\ SHE}$

Cathode: 1) $H_2O + \frac{1}{2}O_2 + 2e^- \leftrightarrow 2OH^- \quad E^o = 0.40V_{\ vs\ SHE}$

2) $2H_2O + 2e^- \leftrightarrow 2OH^- + H_2 \ E^o =- 0.83V_{\ vs\ SHE}$

Overall: 1) $2Na + H_2O + \frac{1}{2}O_2 \leftrightarrow 2Na^+ + 2OH^- \ E^o = 3.11V_{\ vs\ Na/Na^+}$

2) $2Na + H_2O \leftrightarrow 2Na^+ + H_2 \qquad E^o = 1.88V_{\ vs\ Na/Na^+}$

During the charging process, Na$^+$ ions in seawater migrate through the NASICON and are reduced on the negative electrode, while the OER and chlorine evolution reaction (CER) occur at the cathode. During the discharge process, the reverse process occurs with the oxidation of metallic Na at the anode and the ORR and water reduction reaction at the cathode. However, it should be noteworthy that these equilibrium potentials refer to either pH 0 or 14, where ions have unit activity (Fig 2B black dotted lines). Since seawater is a weak base, we have calculated the equilibrium potentials of seawater batteries operating at a pH 8 of seawater. Based on the Nernst equation,

$$E = E^o - 0.05916 \times pH$$

the equilibrium potentials for the OER, ORR, and CER on the positive electrode can be plotted as a function of pH changes as shown in Fig S1 (a Pourbaix diagram). Using the Pourbaix diagram, we can re-estimate the aforementioned theoretical potentials at a pH 8 of seawater.

i) Charging process

Anode: $2Na^+ + 2e^- \leftrightarrow 2Na \qquad E^o = -2.71V_{\ vs\ SHE}$

Cathode: 1) $H_2O \leftrightarrow 2H^+ + \frac{1}{2}O_2 + 2e^- \quad E^o = -0.76V_{\ vs\ SHE}$

2) $Cl^- + 2OH^- \leftrightarrow ClO^- + H_2O + 2e^- \ E^o = -1.24V_{\ vs\ SHE}$

Overall: 1) $2Na^+ + H_2O \leftrightarrow 2Na + 2H^+ + \frac{1}{2}O_2 \ E^o = 3.47V_{\ vs\ Na/Na^+}$

2) $2Na^+ + Cl^- + 2OH^- \leftrightarrow 2Na + ClO^- + H_2O \ E^o = 3.95V_{\ vs\ Na/Na^+}$

ii) Discharging process

Anode: $2Na \leftrightarrow 2Na^+ + 2e^- \qquad E^o = 2.71V_{\ vs\ SHE}$

Cathode: 1) $H_2O + \frac{1}{2}O_2 + 2e^- \leftrightarrow 2OH^- \quad E^o = 0.76V_{\ vs\ SHE}$

2) $2H_2O + 2e^- \leftrightarrow 2OH^- + H_2 \ E^o = -0.47V_{\ vs\ SHE}$

Overall: 1) $2Na + H_2O + \frac{1}{2}O_2 \leftrightarrow 2Na^+ + 2OH^- \quad E^o = 3.47V \; vs \; Na/Na^+$

2) $2Na + H_2O \leftrightarrow 2Na^+ + H_2 \quad E^o = 2.24V \; vs \; Na/Na^+$

In alkaline seawater, the formation of hypochlorite ions (ClO^-) should be considered rather than the CER during the charge process[1]. This hypochlorite formation reaction competes with the OER. The competition can depend on the current density, pH, and local concentration of Cl^- near carbon catalysts. However, the Pourbiax diagram shows that OER is thermodynamically preferred to the hypochlorite ion formation at all pHs because the equilibrium potential of the OER is less than that of the hypochlorite ion formation[1]. If dissolved oxygen is sufficiently involved in the charging process, the same charge/discharge voltage of 3.47 V (vs. Na/Na$^+$) would be expected by reducing the discrepancy between the equilibrium potentials of seawater batteries operating at pH 0 and 14 (Fig 2B green dotted lines). The potential for water reduction reaction also increases to 2.24 V. However, considering the overpotentials for a high current density of 2 mA cm^{-2} and the inherent water reduction reaction, charge potentials of 4.77 V, discharge potentials of 1.97 V, and further dropped to 1.37 V can be observed.

Moreover, we can calculate the theoretical equilibrium potentials of the charging process in acidic solution at pH 5 and 2.

ⅰ) Charging process

Anode: $2Na^+ + 2e^- \leftrightarrow 2Na \quad E^o = -2.71V \; vs \; SHE$

Cathode: $H_2O \leftrightarrow 2H^+ + \frac{1}{2}O_2 + 2e^-$

$$E^o = -0.76V \; for \; pH8, \quad -0.93V \; for \; pH5, \quad -1.11V \; for \; pH2 \; vs \; SHE$$

Overall: $2Na^+ + H_2O \leftrightarrow 2Na + 2H^+ + \frac{1}{2}O_2$

$$E^o = 3.47V \; for \; pH8, \quad 3.64V \; for \; pH5, \quad 3.82V \; for \; pH2 \quad vs \; Na/Na^+$$

The OER potentials are proportional to the acidification of seawater. The overall charging potentials of seawater batteries are expected to be 3.47, 3.64, and 3.82 V at pH 8, 5, and 2, respectively. It also results from the increase in the equilibrium potentials of OER as a function of acidification as shown in Fig S1. It should be noted that all equilibrium potentials are based on the constant values of each chemical potential of H_3O^+ or OH^-. Since the redox reactions of batteries keep changing the chemical potentials of two products in the vicinity of the TFI, the equilibrium potentials of seawater batteries are also variable as redox reactions are in progress. This variation of theoretical potentials as a function of reaction time is considered in the electrochemical tests of 3-electrode configuration in the next paragraph.

2. *Potential behaviors at the cathode of the 3-electrode cell configuration.*

To measure the accurate potential variation of the anode and cathode, we employed a 3-electrode system using a reference electrode of Ag/AgCl, a counter electrode of metallic Na, and a working electrode of carbon felt. The three-electrode system was tested under four conditions: at the charge or discharge state at a pH 8 and 2 of seawater solution, respectively (Fig S7).

At a pH 8 of seawater, the equilibrium potential was theoretically constant 0.55 V vs. Ag/AgCl, assuming the chemical potential (μ) of H_3O^+ and OH^- was not variable during the redox reactions (Fig S7A, Black dashed line). Considering the change of the chemical potential based on the Nernst equation, the theoretical potential on the working electrode increased to 0.85 V for OER due to acidified seawater and decreased to 0.36 V for ORR due to alkalization for 5 h at a pH 8 of seawater (dotted lines). When the high current density of 2 mA was applied to seawater batteries, large overpotentials (solid lines) were observed at 1.163 and 1.44 V from the equilibrium redox potential of 0.55 V (Fig S7A). The theoretical potential was estimated as 0.35 V vs. Ag/AgCl at a pH 2 of seawater due to the different pH value (Fig S7B). This pH effect to the cell potential is represented in the discharge process showing a stable voltage plateau at -0.67 V, which is higher than -0.88 V for the battery operating at pH 8 seawater. However, the potential variation was severe at the charging process. The cell potential abruptly increased to the limited condition of 4.08 V after 0.47 h as shown in Fig S6B.

It should be noted that the potential profiles measured by the 3-electrode configuration are consistent with those of the 2-electrode system as shown in Fig 2B and S6. The potential correspondence of two systems indicates that the potential variation of the counter electrode is negligible, suggesting that the redox reaction of the working electrode was dominant for the full-cell experiment. Theoretically, the potential deviation of the counter electrode is expected to be 0.002 V during a single reaction for 5 h at 2 mA. Since reduced/oxidized Na^+ ions at the negative electrode are much less than the initial Na^+ ions in the organic electrolyte, a logarithm value of the high Na^+ concentration in the organic electrolyte (1 M) is nearly constant, resulting in low potential variation according to the Nernst equation. Thus, the overall potential difference of 0.004 V by the counter electrode is negligible compared to the potential (0.49 V) at the working electrode. It indicates that most of the potential information of seawater batteries results from the OER/ORR on the carbon felt rather than the oxidation/reduction on metallic Na. Therefore, the electrochemical reactions on carbon felt are dominant to the overall voltage profiles.

Ions	Ion concentration (mg/L)	
	Sample seawater	Standard seawater[2]
Na^+	9,803	10,780
Cl^-	19,034	19,350
K^+	581	400
Mg^{2+}	1,335	1,280
Ca^{2+}	404	410
$SO_4^{\ 2-}$	2,735	2,710
Total	33,892	34,930

Ionic conductivity: 1.2269 S/cm

Supplementary Table

Table S1. A comparison of the chemical compositions between our sample and standard seawater.

Supplementary Figures

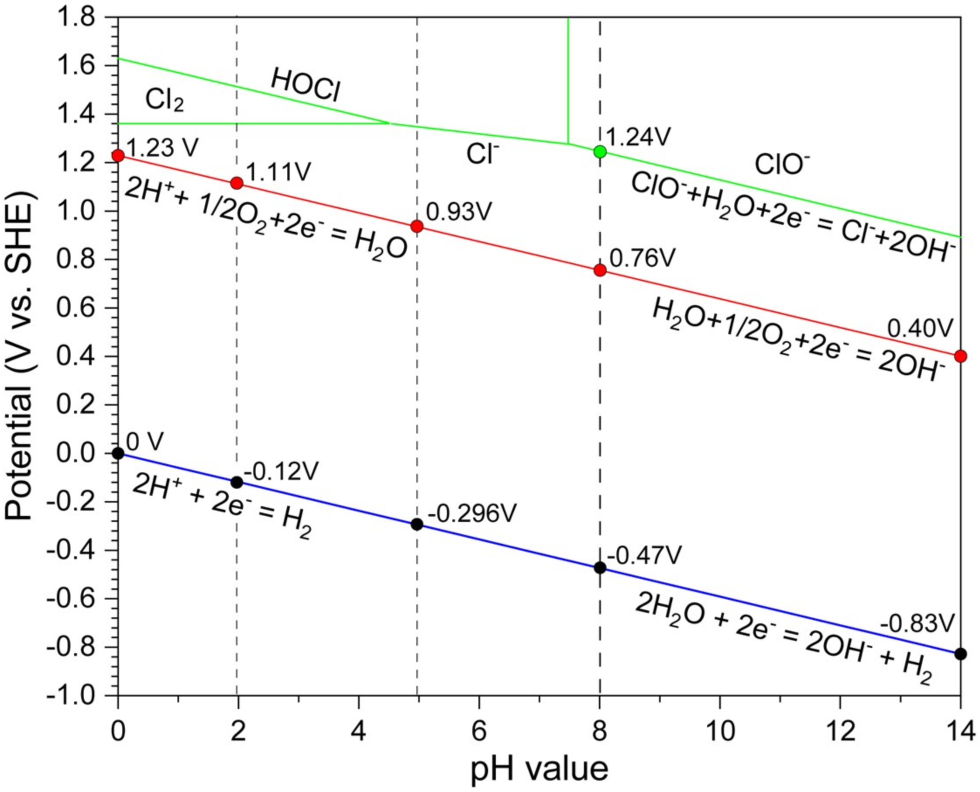

Fig S1. Calculated Pourbaix diagram for seawater at a standard room temperature and ambient pressure (298 K, 1 bar).[3] The electrochemical water stability is ranged between the red line for ORR and the black line for water reduction. The equilibrium line for the chlorine stability is plotted for 0.54M of total chlorine concentration.

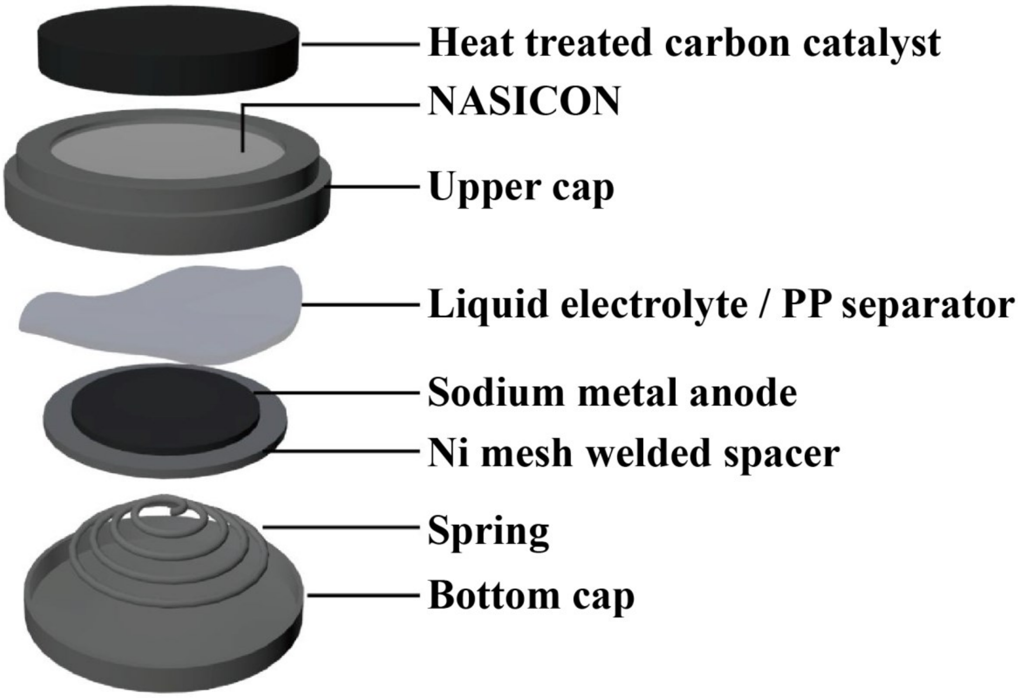

Fig S2. Structure of the coin-type seawater battery cell. A coin cell consists of the NASICON, top and bottom caps, PP separator soaked with a liquid electrolyte, sodium metal anode on Ni mesh spacer. The heat treated carbon catalyst is immersed in the seawater on the cathode side (illustrated in Fig 1A)

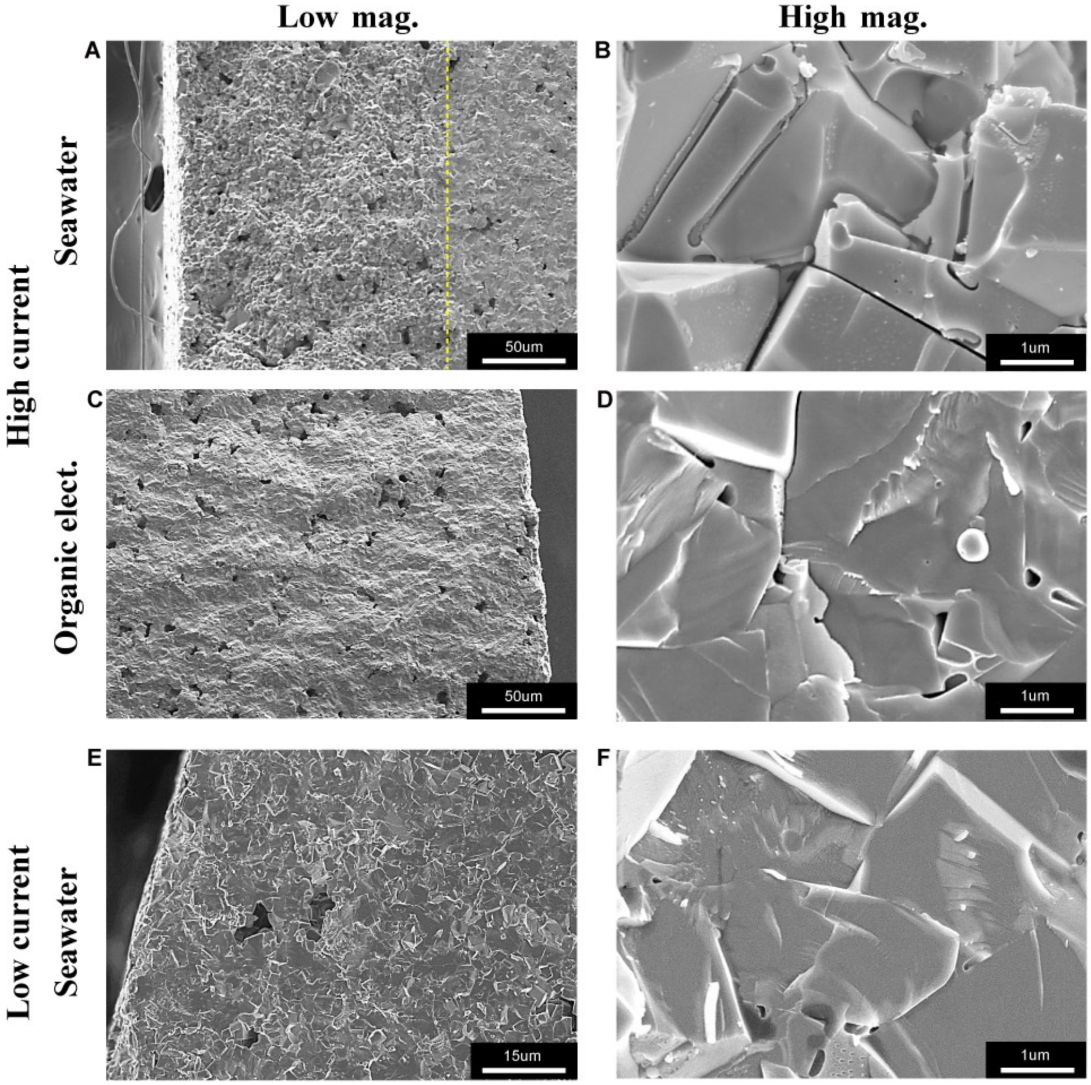

Fig S3. Cross sectional SEM images of the electrochemically reacted NASICON. Low and high magnification NASICON images on the left and right column, respectively. (A, B) Seawater contacted side after the repeated charged and discharged reactions at 2 mA cm^{-2} for 10 h. (C, D) The organic electrolyte contacted side views of the same NASICON in (A, B). (E, F) The seawater contacted side views of the NASICON reacted at a low current density 0.15 mA cm^{-2} for 5 h. No degradation is observed even at seawater contact side, where the morphology is still the same as the pristine NASICON as shown in Fig S3A.

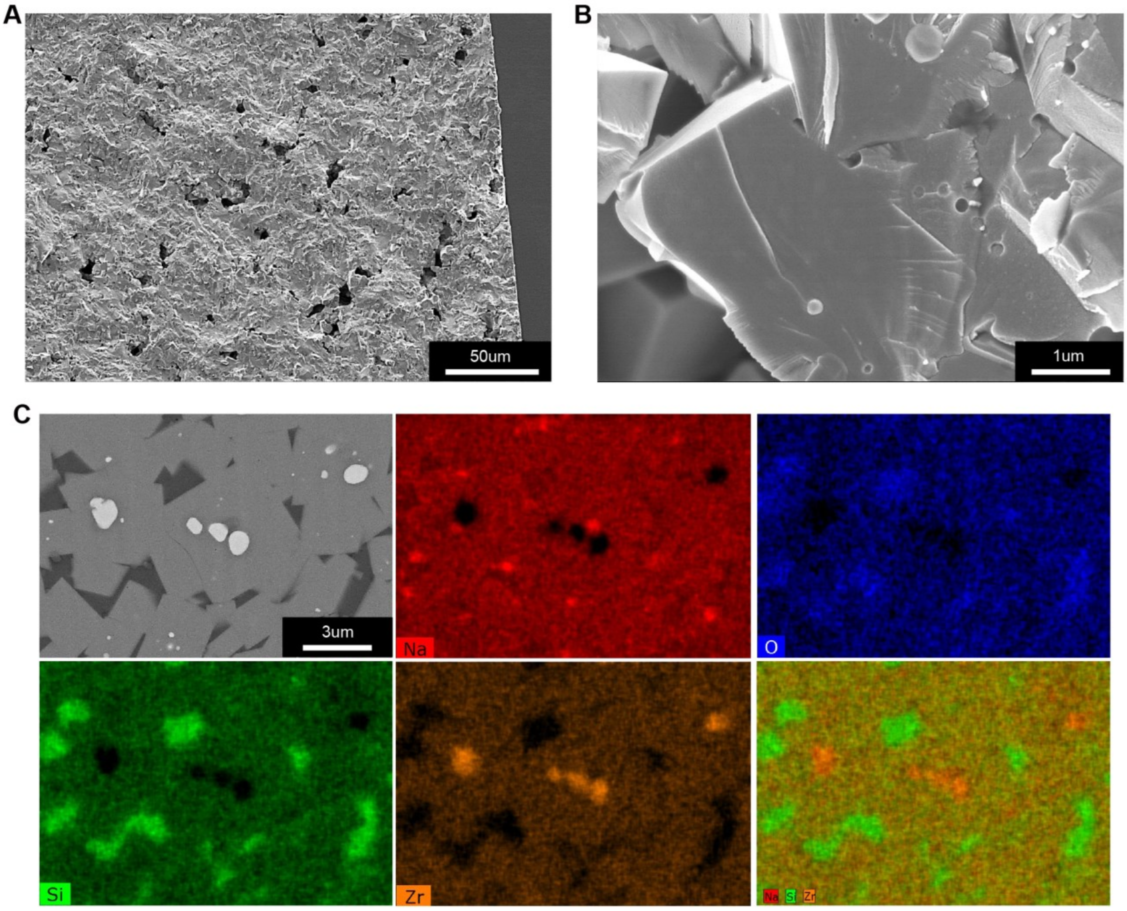

Fig S4. Characterization of the cross sectional morphology of the pristine NASICON. (A, B) Low and high magnification SEM images of the pristine NASICON. (C) SEM-BSE image of the ion-milled pristine NASICON and EDS mappings of every comprising element; NASICON main phase (gray), Si and Zr rich phase (dark gray and white). It shows the clear grain boundaries between each phase without micro-cracks.

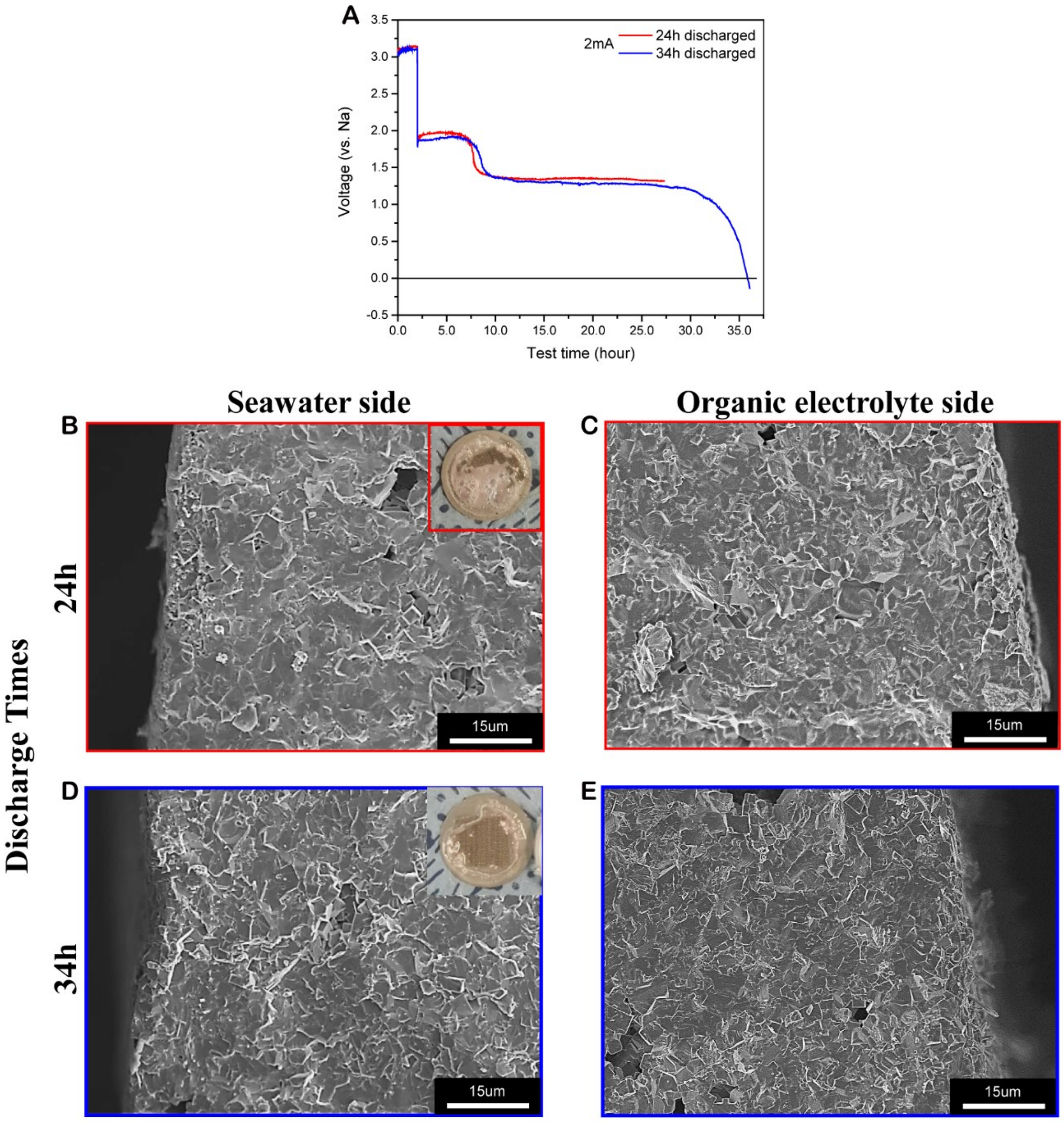

Fig S5. Discharging voltage profiles and cross sectional SEM images on the seawater side (left column) and organic electrolyte side (right column). (A) Discharging voltage curves for 24h and 34h after initial rest time of 2 h. The sudden voltage drops result from an exhaustion of the amount of dissolved oxygen. The water molecules are only associated with a discharging process.[1] (B~E) The seawater and organic electrolyte contacted sides after discharging for 24h and 34h and optical microscopy image of remained sodium metal foil (inset). All images indicate that the NASICON was not deteriorated, and thus the discharge process does not damage the NASICON. The sodium metal foil is stripped from the Ni mesh.

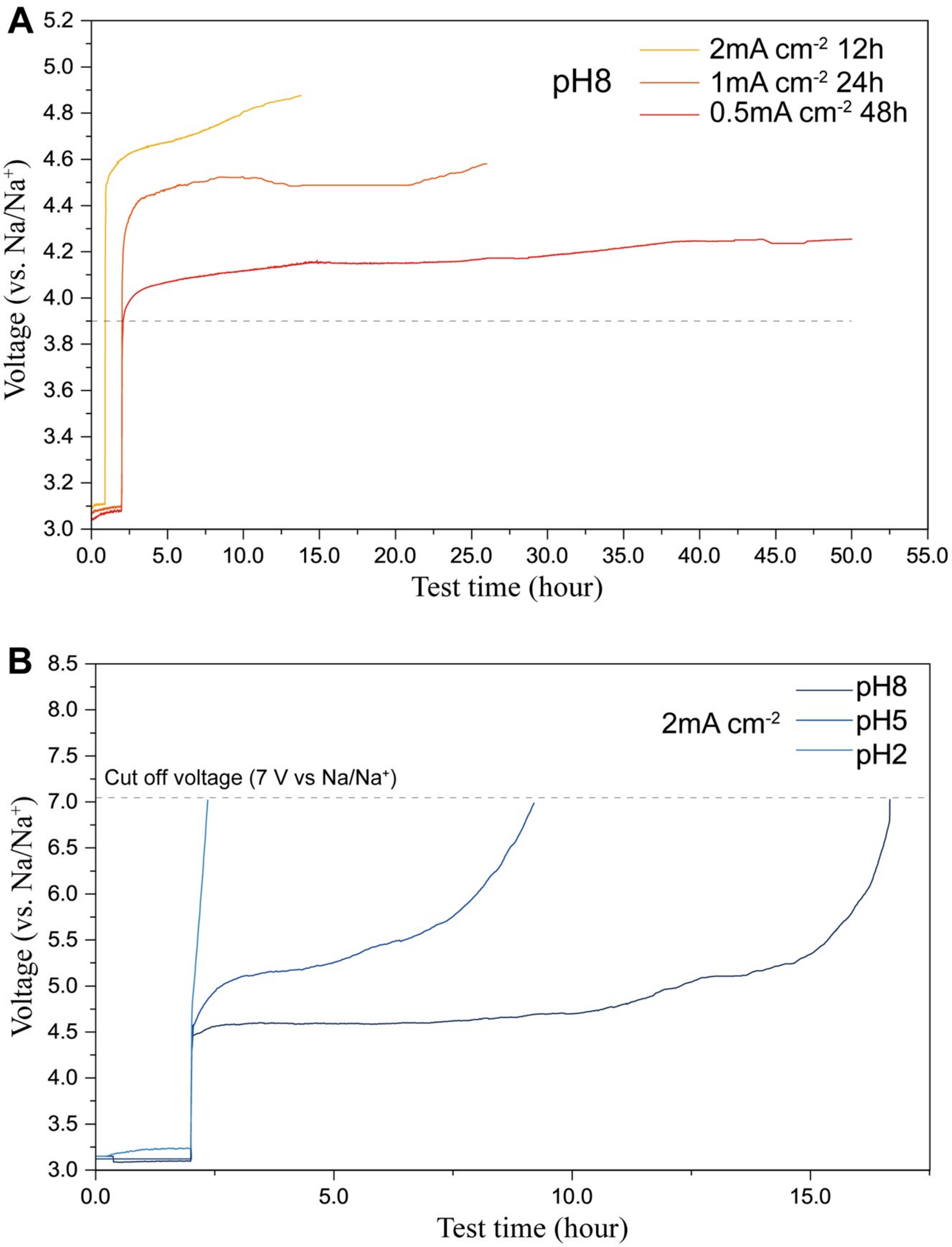

Fig S6. Comparison of voltage curves during the charging process. (A) Galvanostatic testing with various current densities from 0.5 to 2mA cm^{-2}. The amounts of plating Na plating on the anode were controlled to be constant by altering the charging time (48h, 24h, and 12h). (B) A severe polarization occurred at the different pH values of seawater from pH 8 (Pristine seawater solution) to pH 2 (Highly acidified) in the same current density of 2mA cm^{-2}. We set a cut off condition up to 7 V. The voltage plateau becomes shorter with an acidification of the seawater and eventually cannot be found in pH 2 solution.

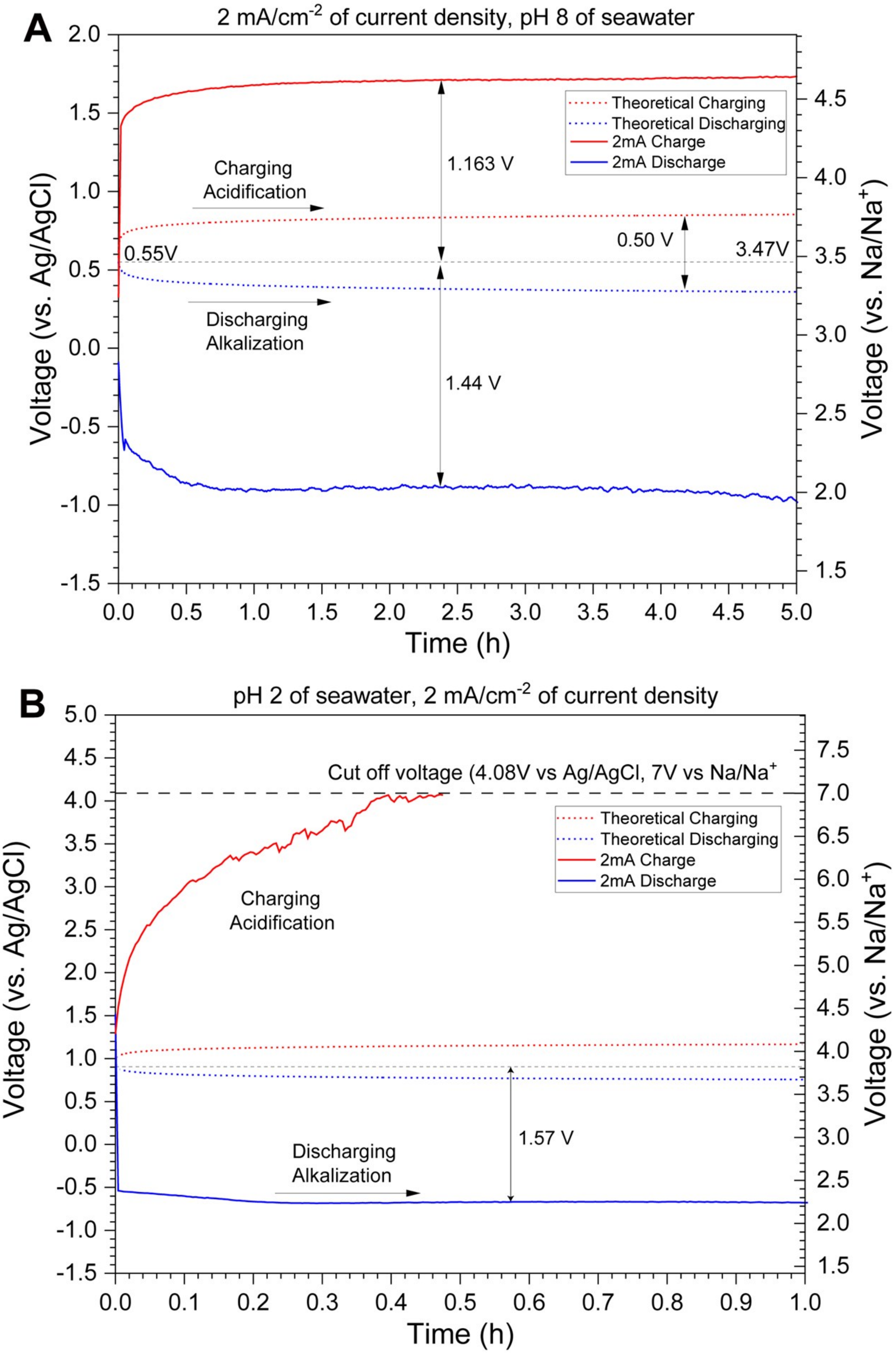

Fig S7. Electrochemical voltage profiles of the working electrode in 3-electrode cell configuration with a Ag/AgCl reference electrode. The equilibrium potential and cell potential are represented with dashed and dotted lines, respectively. (A) The voltage profiles of the cathode reaction occurring at a pH 8 and (B) pH 2 of seawater.

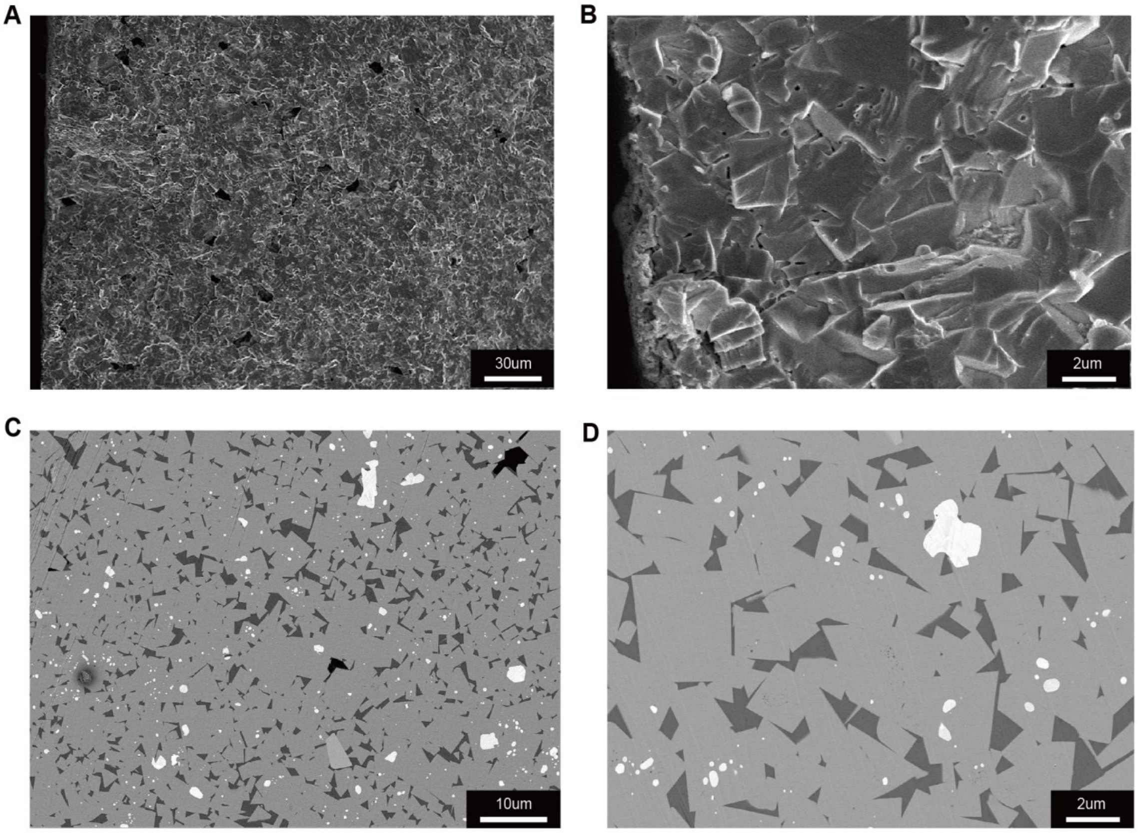

Fig S8. The cross sections of the NASICON immersed for a more than 1 year in acidified seawater (pH 2). Low and high magnification SEM images on the left and right column, respectively. (A, B) SE mode images. (C, D) BSE mode images of the ion-milled NASICON near the contact surface. All images reveal that the NASICON is physically stable in the harsh acidic seawater.

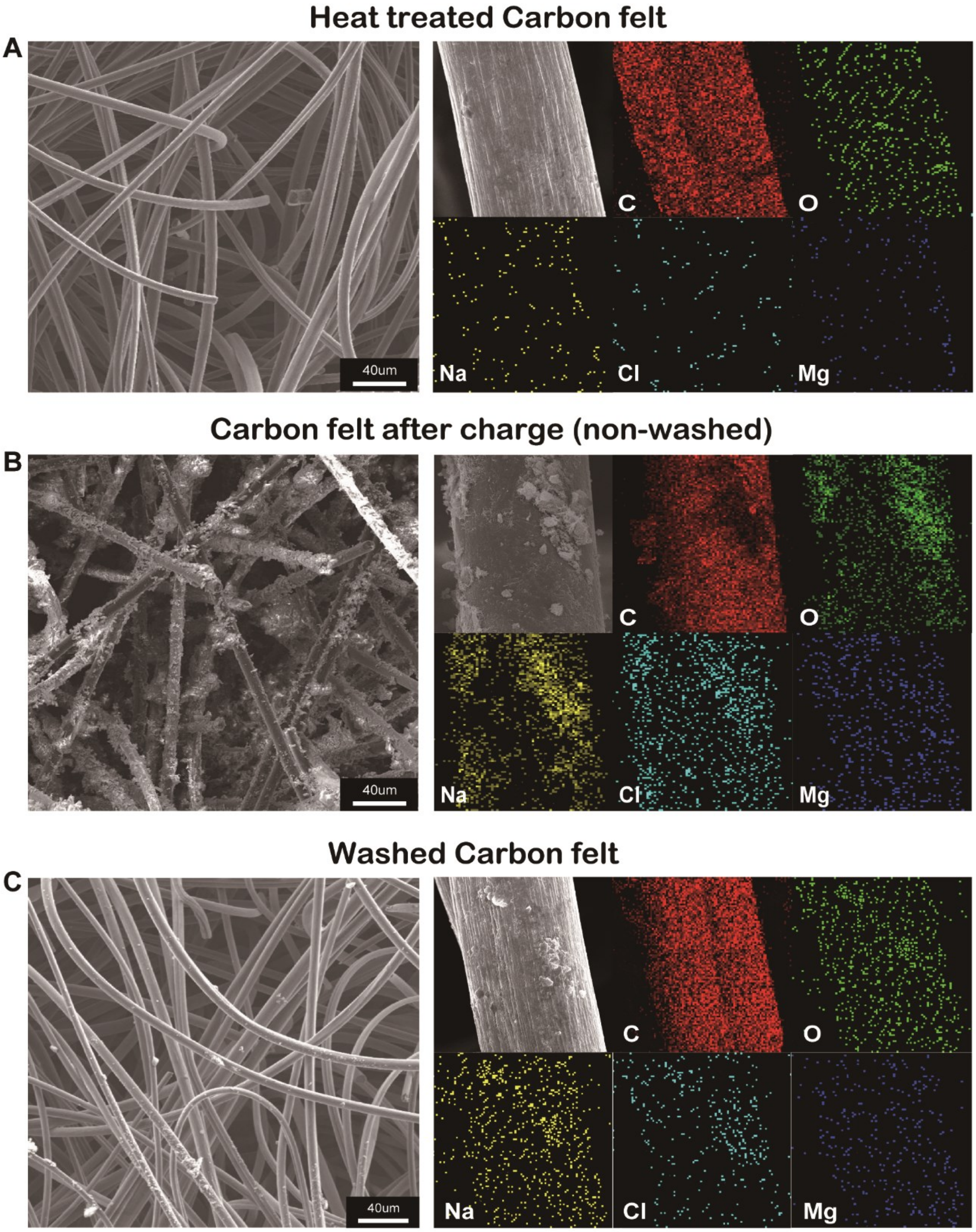

Fig S9. The carbon felt SEM images and EDS mapping analysis after the cell is charged (OER). All area observed here is the interface in contact with the NASICON. (A) The surface of the carbon felt catalysts heat treated at 500°C for 5 hours. The surface is smooth without contamination or cracks. (B) The dried carbon felt catalyst surface after a seawater cell was charged. The material was not cleaned with D.I. water. The precipitates from the seawater are smeared on the surface. (C) A washed carbon catalyst shows that its morphology has been maintained, similar to the heat treated carbon felt.

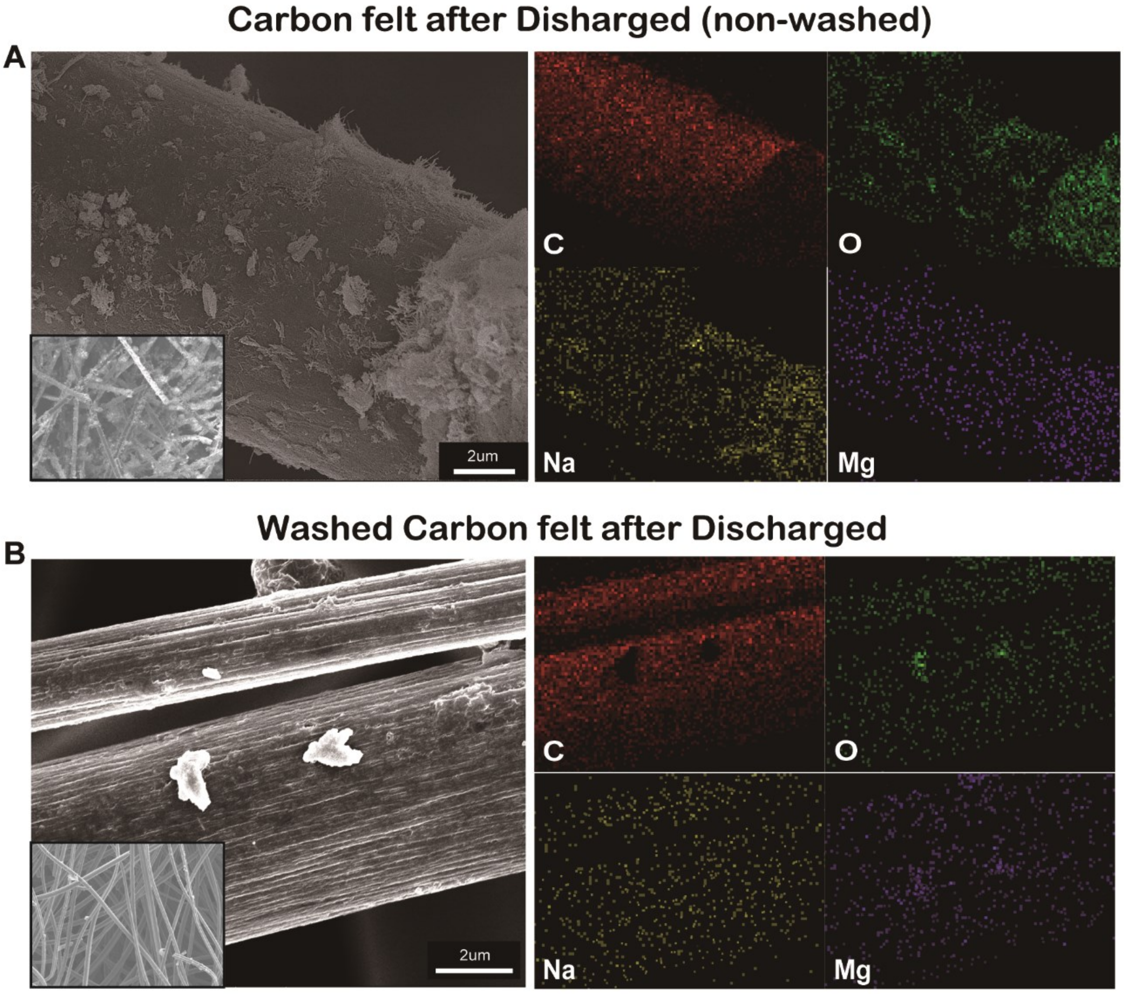

Fig S10. The magnification of SEM images and EDS mapping for carbon felt after discharging at 2 mA cm^{-2}. (A) The surface of carbon felt, which was not cleaned by D.I. water, shows the precipitates containing similar morphologies and chemical compositions compared to the charged sample. (B) Washed carbon felt shows that the carbon catalysts are chemically and electrochemically stable in the acidic and basic seawater solution with a reductive condition. Although Mg-contained insoluble salts are still observed on the carbon catalysts, most of the precipitates are easily dissolved in an aqueous media. The small number of insoluble salts would not disturb the ORR process.

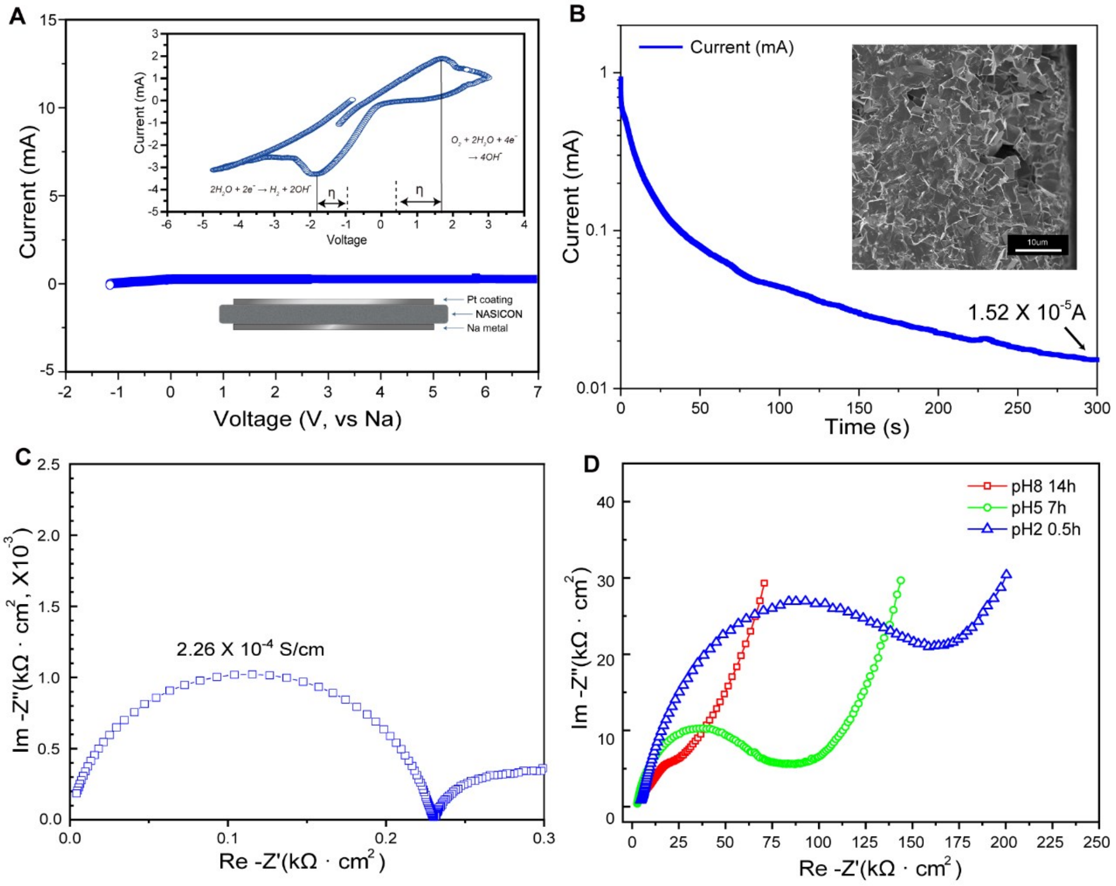

Fig S11. Electrical characterization of the NASICON. (A) Linear sweep voltammetry (LSV) of the pristine NASICON and the full cell of seawater batteries (inset). The solid electrolyte is typically positioned between a working (Pt) and a reference metal (Na) electrode. The inset graph shows net current densities derived from the decomposition of water molecules in the full cells of seawater batteries. The decomposing reactions take place on the carbon catalyst (a working electrode) that also serves as a current collector. (B) The current-measuring time curves of the Pt/NASICON/Pt cells under DC polarization at 2V. The current decreases and reaches a steady state at 1.52×10^{-5} A. (C, D) Nyquist plots of the pristine NASICON and charged NASICON in the pH-adjusted seawater solution.

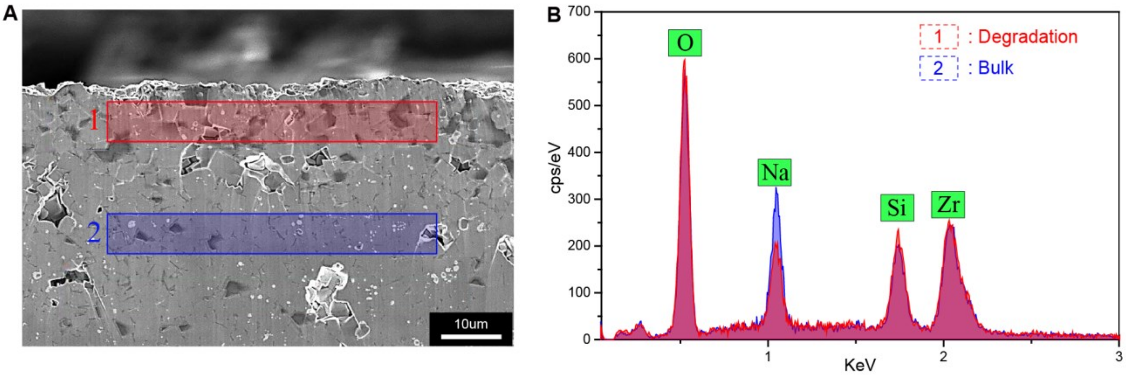

Fig S12. The comparison of elemental distribution in the micro-cracked region of a NASICON pellet and inner bulk region. (A) A cross-sectional BSE-SEM image after an ion milling process. (B) The EDS peaks of the degraded NASICON part (red color, 1) and inner sites (blue color, 2). The sodium content is deficient in the damaged region.

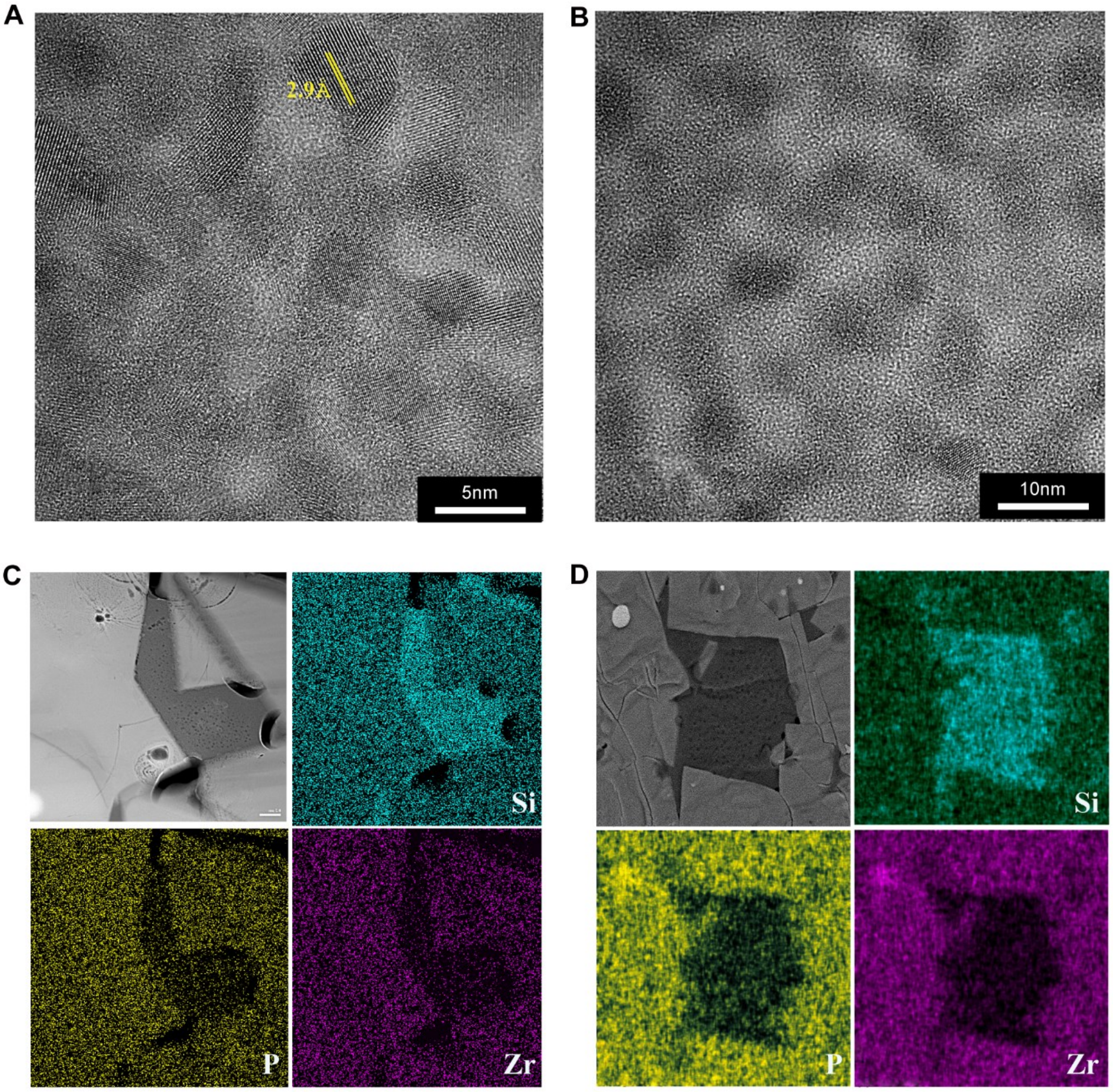

Fig S13. (A, B) High-resolution TEM images of the polycrystalline pristine NASICON and amorphous Si rich phase. The distance between (116) planes is around 2.9Å which is larger than damaged NASICON. (C, D) The EDS mappings of a HR-TEM image and a SEM image at the amorphous Si-rich phase for elements Na, Si, P, and Zr.

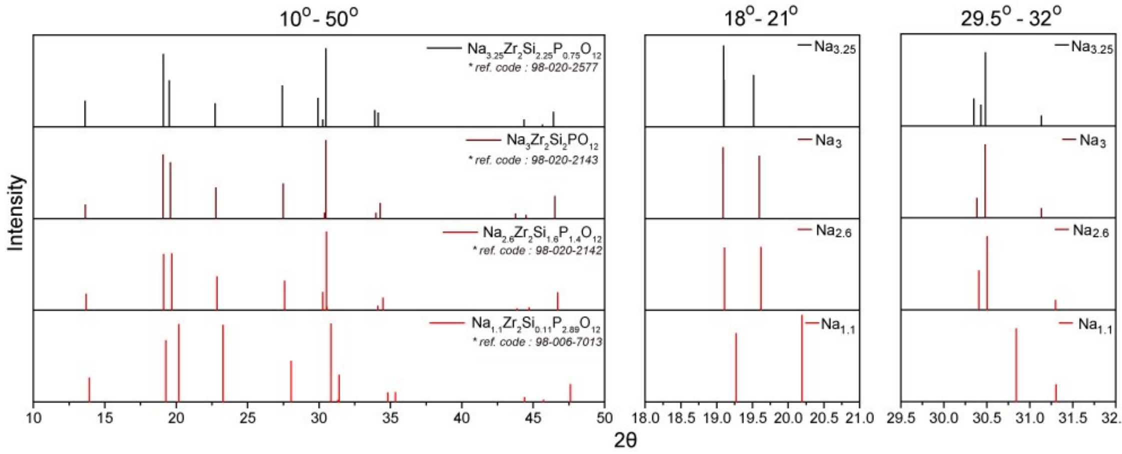

Fig S14. The comparison of the NASICON reference family $(Na_{1+x}Zr_2Si_xP_{3-x}O_{12})$ at specific ranges. (A) 10°~50°, (B) 18°~21° and (C) 29.5°~32°. The ratio of the first to second peak at 18°~21° has been decreased and shifted toward the higher angle with extreme extraction of sodium until $Na_{1.1}$ stoichiometry. It corresponds to a deficiency of Na^+.

References

1. Dionigi, F., Reier, T., Pawolek, Z., Gliech, M., Strasser, P. *ChemSusChem,* 2016, **9**, 962–972.

2. Millero, F. J., Feistel, R., Wright, D. G. McDougall, T. J. *Deep. Res. Part I Oceanogr. Res. Pap.* 2008, **55**, 50–72.

3. Pourbaix, M. 1974, doi:10.1016/0022-0728(67)80059-7.